EARTH'S CRYOSPHERE
SCIENTIFIC JOURNAL

Earth`s Cryosphere, 2017, vol. XXI, No. 4, pp. 48–62 **http://earthcryosphere.ru/**

SNOW COVER AND GLACIERS

DOI: 10.21782/EC2541-9994-2017-4(48-62)

HIGHLY DYNAMIC ROCK GLACIERS OF TIEN SHAN

A.A. Galanin[1,3], V.V. Olenchenko[2], I.I. Khristoforov[1], E.V. Severskiy[1], A.A. Galanina[3]

[1] *Melnikov Permafrost Institute, SB RAS, 36, Merzlotnaya str., Yakutsk, 677010, Russia; agalanin@gmail.com*
[2] *Institute of Petroleum Geology and Geophysics, SB RAS, 3, Acad. Koptyuga ave., Novosibirsk, 630090, Russia; olenchenkovv@yandex.ru*
[3] *Northeastern Federal University, 58, Belinskogo str., Yakutsk, 677000, Russia*

A comprehensive study based on electrical resistivity tomography and GPR methods, geothermal monitoring and the stable isotopes analysis of glacial runoff has established that the most active frontal parts of Gorodetsky rock glacier in the Northern Tien Shan are thawed and substantially free of ground ice. The fast moving frontal parts of Gorodetsky rock glacier are composed of a mixture of coarsely fragmented debris, blocks of metamorphic ice and thixotropic sand- and clay-loamy filler. The input of fine-graded component from the glacial runoff infiltration and accumulates in the pores and voids of rock glacier, results in a gradual change in its physical properties (volume density, plasticity). Dynamics of such rock glaciers does not obey Glen's law for viscous flow, and the presence of ground ice does not exert any significant effect on their inner deformations. Rheology models for such landforms can be based on the behavior of pseudoplastic (non-Newtonian) fluids and thixotropic systems. The lichenometry and Schmidt Hammer Test data provided a basis for establishing four different age generations of rock glaciers. These generations correlate well with Late Holocene oscillations of mountain glaciers in the Northern Tien Shan, which bears clear evidence of strong historical and genetic relationships between common glaciers and rock glaciers.

Rock glaciers, electrical resistivity tomography, ground penetrating radar, lichenometry, Schmidt Hammer Test, glacial mudflow, alpine permafrost, Tien Shan, Central Asia, Glen's law

INTRODUCTION

Of the studied Northern Tien Shan glaciers, Gorodetsky rock glacier is probably the largest whose length is about 3.5 km. It is located at the Bolshaya Almaatinka river headwaters in the axial part of the Zailiysky Alatau ridge (altitudinal range: from 3140 to 3450 m a.s.l.). The glacier source area accommodates several intensively shrinking corrie glaciers, including the largest, namesake Gorodetsky glacier. Various aspects of structure, morphology and dynamics of Gorodetsky rock glacier and other types of glacial landforms in the region have been recurrent themes of discussion for more than half a century, which laid the foundation for the emerging national scientific school on rock glaciers [*Iveronova, 1950; Palgov, 1957; Glazovsky, 1977; Gorbunov and Titkov, 1989; Gorbunov et al., 1992; Gorbunov and Severskiy, 2000; Marchenko, 2003; Gorbunov, 2006, 2008*]. However, the amount of research on rock glaciers in Russia and in the territory of FSU countries is exceedingly small compared with European countries and the American continent [*Barsch, 1996; Haeberli et al., 2006; Galanin, 2010*], which is aggravated by the instrumental base development remaining to be at the level of the 1960–1970s [*Gorbunov, 2006, 2008; Galanin, 2009*].

A new surge of interest in rock glaciers emerged in the 21st century in part accounts for their specific response to the ongoing global climate change. Against the backdrop of the intensively shrinking ordinary glaciers, many rock glaciers have grown in size and are actively advancing [*Glazovsky, 1977; Marchenko, 2003; Vilesov et al., 2006; Galanin, 2009*]. The mechanisms for activation of rock glaciers creep in many aspects contradict the concepts of their structure and rheology that established themselves in the first half of the 20th century. Back in 1998, the International Permafrost Association (IPA) launched the "Permafrost Creep and Rock Glacier Dynamics" program guided by W. Haeberli, with an aim to provide an overview of the late-20th-century studies on rock glaciers. In the published report, W. Haeberli and colleagues concluded that despite the huge amount of accumulated evidence, "the creation of a unified physical model for permafrost found in alpine rock glaciers, to represent creep and failure in variable temperature regimes remains a distant goal" [*Haeberli et al., 2006, p. 203*].

In 2012–2014, the authors studied Gorodetsky rock glacier in the Northern Tien Shan [*Galanin et al., 2015*] using a complex of modern technologies, which included: electromagnetic tomography (ERT) and ground penetrating radar (GPR); glacier run-off water temperature monitoring by automatic geothermal loggers; analysis of the isotope composition of meltwater runoff and fossil ice; route and remote mapping using satellite imagery and digital elevation models (DEM); study of natural outcrops in the walls of thermo-erosion subsidence and cliffs; determination of relative and absolute age on the basis of lichenometry and residual strength test.

RESULTS OF INSTRUMENTAL OBSERVATIONS OF GORODETSKY ROCK GLACIER IN 2013–2014

Figure 1 represents a schematic profile of Gorodetsky rock glacier derived from the interpretation of satellite images and field surveys data.

Geophysical studies of Gorodetsky rock glacier were conducted on all the profiles by ERT coupled with GPR methods. The survey profiles were located along and across the rock glacier runoff system (Fig. 1). The lengths of profiles were: transverse (Pr1) – 955 m, longitudinal (Pr2) – 1075 m. These are the longest ERT profiles known in the world practice of geophysical studies of rock glacier [*Francou et al., 1999; Fabre et al., 2001; Farbrot et al., 2005; Maurer and Hauck, 2007*]. Another 235 m long profile (Pr3) was located above the natural exposure of buried metamorphic ice. The data obtained from ERT measurements along the Pr3 profile were used as reference data for interpreting sections for the remaining profiles, employing "Scala-48" as ERT measuring instrument, a multi-electrode station developed at Trofimuk Institute of Petroleum Geology and Geophysics SB RAS. The sequence of electrodes connection corresponded to a Schlumberger symmetric electrode array configuration, with maximum electrode spacing 117.5 m. The measurement interval along the profile was 5 m. We used saline solution to improve the contact between electrodes and medium, which allowed reducing the resistance-to-ground from 100–300 to 10–30 kOhm. The acquired ERT data were processed using Res2Dinv softaware [*Loke, 2009*]. Differentiation between frozen and thawed rocks was made on a key assumption that resistivity of the former is abnormally high (hundreds and thousands of times), unlike the latter [*Recommendations..., 1987;*

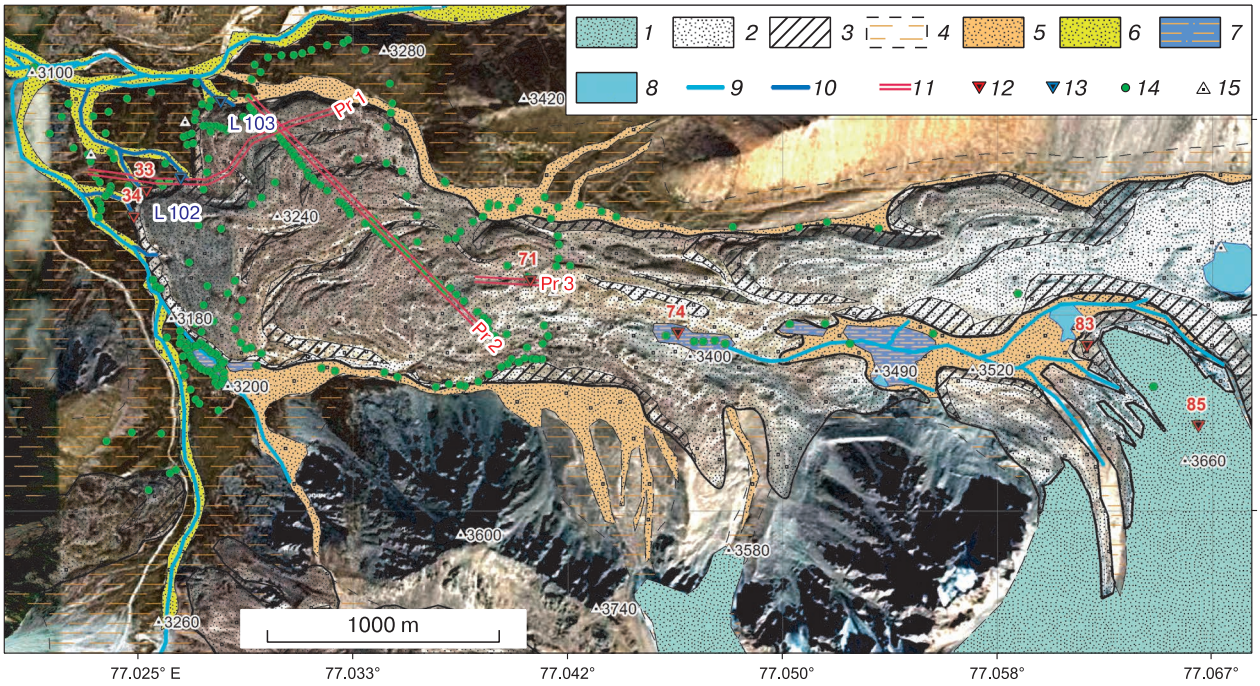

Fig. 1. Structural elements of Gorodetsky rock glacier, profile and local observation points positioned on the satellite image:

1 – glaciers; *2* – gravelly-blocky-structured surface of rock glacier; *3* – steep debris slopes; *4* – boulder-pebble-clay loamy ground moraine of late Pleistocene glaciation; *5* – boulder-pebbly dry stream beds of glacial drainage system; *6* – boulder-pebbly stream bed and floodplain of permanent watercourses; *7* – drained stream beds of periglacial lakes with banded sediments; *8* – contemporary periglacial lakes; *9* – high turbidity water courses; *10* – low turbidity watercourses, filtered from under the rock glacier; *11* – geophysical profiles (from ERT and GPR data) and their numbering; *12* – ice and water sampling points for $\delta^{18}O$ and δD; *13* – automatic loggers for temperature monitoring of meltwater runoff and their numbering; *14* – lichenometric dating and residual strength test sites; *15* – absolute elevation marks.

Frolov, 1998]. It was also taken into consideration that resistivities of frozen rocks and ice are temperature-dependent, and that resistivity increases as temperature decreases.

The GPR sounding was conducted using the OKO-2 georadar with linear ABDL-Triton unshielded antennas with 50 MHz central frequency and a dual-frequency antenna unit with 150 and 400 MHz central frequencies.

Given that investigating rock glacier along large distance profiles is additionally challenged by the difficult-to-traverse terrain, the technique was applied to surveying short, 50 m intercepts which, subsequently, were incorporated into the final profile. The measurements were performed with the following preset survey parameters: time-frequency signal analysis (800 ns signals); accumulation of signals at each observation point, OP (32); average dielectric constant equals 6. For the GPR data processing and interpretation we used Geoscan-32 software, with involvement of the main criterion for isolating water-logged zones based on intense low-frequency reflected signal, appearing on radargrams in the form of wide blacked bands. Normally, the top of frozen rocks and bedrock are distinguished on radargrams by a clear equal phase line of the reflected wave [*Vladov and Starovoytov, 2004; Kneisel et al., 2008*].

Geophysical reference profile Pr3 is laid over the transit zone of the rock glacier in the side-wall of a large thermokarst ellipsoidal depression 90–100 m in size (Fig. 1, OP 71). A water body formed on its bottom is about 50 m in diameter. Its shores are bristling with unstable large blocks of granite.

The water in the lake is turbid because of glacial 'flour'. A natural outcrop on the left bank of the water body is represented by a monolithic-frozen escarp up to 20 m in height, and about 70 m long which was used as a reference section (Fig. 2, *a*, *b*). At the base of the outcrop there are deep flat niches sinking under the lens at the lake water level. The observed phenomena during the field works included draining of "vadose water", systematic slumping and collapse of the gravelly-blocky surface layer from the escarp edge directly to the lake. A metamorphic ice lens, 16–17 m thick, overlain by the 1.0–1.5 m thick loose gravelly debris cover is exposed in the outcrop (Fig. 2, *a*, *b*).

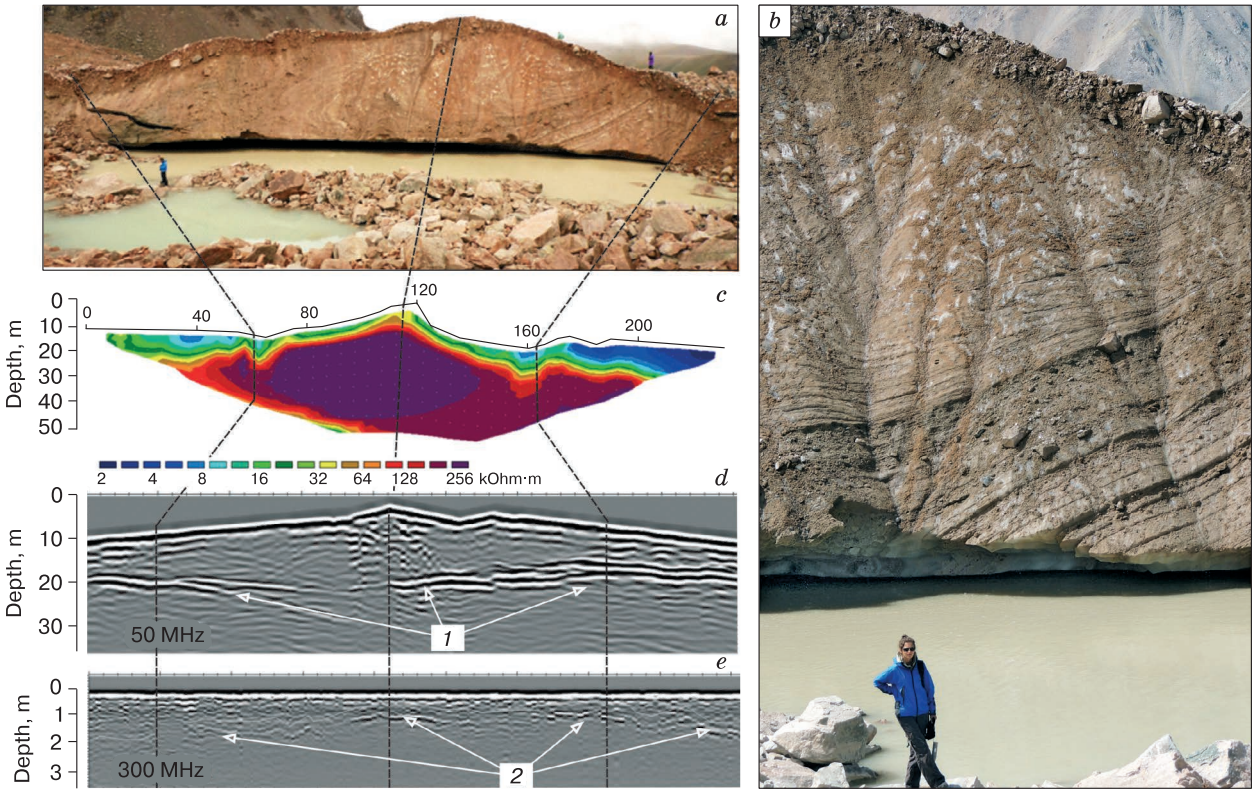

Fig. 2. Pr3 geophysical profile laid along the thermoerosion cliff edge, with outcropping fossil block of metamorphic (firn) ice in the middle part of Gorodetsky rock glacier.

a – wall of thermoerosion subsidence and correlation lines of geophysical profiles (dashed lines); *b* – close-up of the right side of thermoerosion cliff with a clearly visible syngenetic stratification and glacio-dislocations (folded structure) in a fossil block of metamorphic ice; *c* – geoelectric section according to ERT data; *d*, *e* – radargrams obtained from GPR data (frequency: 50 and 300 MHz); *1* – radio waves reflection zones (frequency: 50 MHz) corresponding to the base of ice block; *2* – reflection zones corresponding to the upper surface of ice block (frequency: 300 MHz) from the top of ice block.

The ice is characterized by annually persistent layers with thickness varying between 5 and 20 cm creased into an asymmetric synclinal (spoon-shaped) fold whose axis is oriented down the valley. This proves the ice to be of firn origin and its subjected to subsequent metamorphism in the body of a large glacier. At the lens top, which coincides with the boundary of the seasonally thawing layer (active layer, AL), ice bedding planes tend to be truncated at an angle of about 45°. The lens edges pinch out at low angle, gently submerging into a loose uncemented gravelly-blocky mass. The contact between the lens top and gravelly surface cover appears of contrasting character. The contact zone is contoured by a 10–20 cm thick, sand- and clay-loamy rim. The left edge of the lens is dissected by a gently inclined, freshly formed crevasse, filled with loose gravelly-blocky material.

Several other outcrops of fossil metamorphic ice with thickness up to 15 m are established in the upper part of the rock glacier. All of them are relict blocks of "dead ice" of metamorphic origin, severed from the paleoglacier during its retreat and buried beneath the surface gravelly-block moraine. In all the studied sections, no signs of epigenetic ice formation were found, specifically, of congelation ice, capable of cementing the clastic matrix of rock glacier.

The ERT data-based geoelectric section along the profile Pr3 is shown in Fig. 2, *c*. The minimum resistivity values (ca. 2 kOhm·m) are characteristic of the unconsolidated debris cover with a filler overlying the frozen deposits in the right part of the profile (175–235 m). Whilst higher resistivities (8–16 kOhm·m) feature relatively young sediments of debris cover with minimum amount of filling material. The glacier nucleus is distinguished by anomaly in resistivity (50–250 kOhm·m), while resistivity at the top of ice lens is 10–20 kOhm·m, which may be accounted for its temperature being close to 0 °C. In the near-surface part, the detected active layer with a thickness ranging from 1.5 to 5–7 m has a resistivity of 2–8 kOhm·m. At 65 and 160 m points, the low resistivity anomalies of a characteristic shape are distinctly manifest, which is associated with the filtration channels, inasmuch as noise of the water was heard over them during the surveys. The ERT results has thus demonstrated on the reference profile that the resistivity distribution in the section reflects the internal structure of the rock glacier (Fig. 2).

The results of the 2D inversion of the ERT data contain three-dimensional distortions due to the effect of ground-air lateral interface in the steeply dipping side of the outcrop, which leads to a general increase in the model resistivity. At the same time, results of the model – real section correlation show that the obtained resistivity distribution pattern reflects the internal structure of the rock glacier perfectly well. Figure 2, *d* shows a radargram obtained from the low frequency (50 MHz) GPR surveys conducted at depths of 30–40 m, with dielectric permittivity of the medium averaging $\varepsilon = 6$. As is seen from the GPR data, the occurrence depth of the rock glacier bed is identified on the radargram as a clearly distinguished reflector at a conditional (for a given ε) depth of 20 m. At high frequencies (300 MHz), the GPR method provides information on thickness of the unconsolidated debris cover and the depth of permafrost table (Fig. 2, *e*). The debris cover sediments are distinguished on the 300 MHz frequency radargram by characteristic rereflections creating a high-frequency noise in the section up to a depth of 1.5–2 m. The upper limit of glacial ice is identified along the long equal phase line of the reflection, below which the wave field attenuates.

Figure 3, *b* represents the longitudinal geoelectric section of the rock glacier along the Pr2 profile, which was laid along the rock glacier axis, from the edge of the front slope (Fig. 1). The ERT results interpretation was done taking into account the Pr3 reference profile data and the VES (vertical electrical sounding) results for rock glaciers in the Bolivian Andes. It has been established that resistivities lower than 44 kOhm·m correspond to melted zones of rock glaciers with a temperature of ca. 0 °C. Water-logged melted zones have lower specific resistivity varying between 0.5 and 15 Ohm·m. At the sites of rock glaciers where ice-cement fraction constitutes more than 30 % of their volume, resistivity tends to be greater than 80 kOhm·m [*Francou et al., 1999; Fabre et al., 2001*].

The ERT survey results showed that the average resistivity of high-ohmic rocks of Gorodetsky rock glacier increases progressively from the first tens to the first hundreds of kOhm·m from the talus accumulation at the foot of its frontal slope upwards along the valley. Contrasting alternation of low and high resistivity regions feature the geoelectric section of the marginal, most highly dynamic, part of the rock glacier. Up the valley, the high ohmic regions grade into continuity, and their resistivity grows. An increase in the resistivity across the section upward along the valley is presumably associated either with increased ice content of the sediments, or with decreased temperature of ice.

The abrupt changes in the resistivity and structure of the geoelectric section along the Pr2 profile correlate well with the boundaries of the variously aged generations of rock glacier. Sediments in the oldest, first generation (Fig. 3, *b*) are characterized by extremely low resistivities (0.5–15 kOhm·m), except for slightly anomalous resistivity (<100 kOhm·m), most likely attributed to small lenses of metamorphic ice. The glacier bed within the bounds of this generation is completely melted and saturated with water, which is characterized by low resistivity of rocks (<5 kOhm·m) and intense reflection events in this interval of the profile (the dark area on the radargram, cf. Fig. 3, *c*).

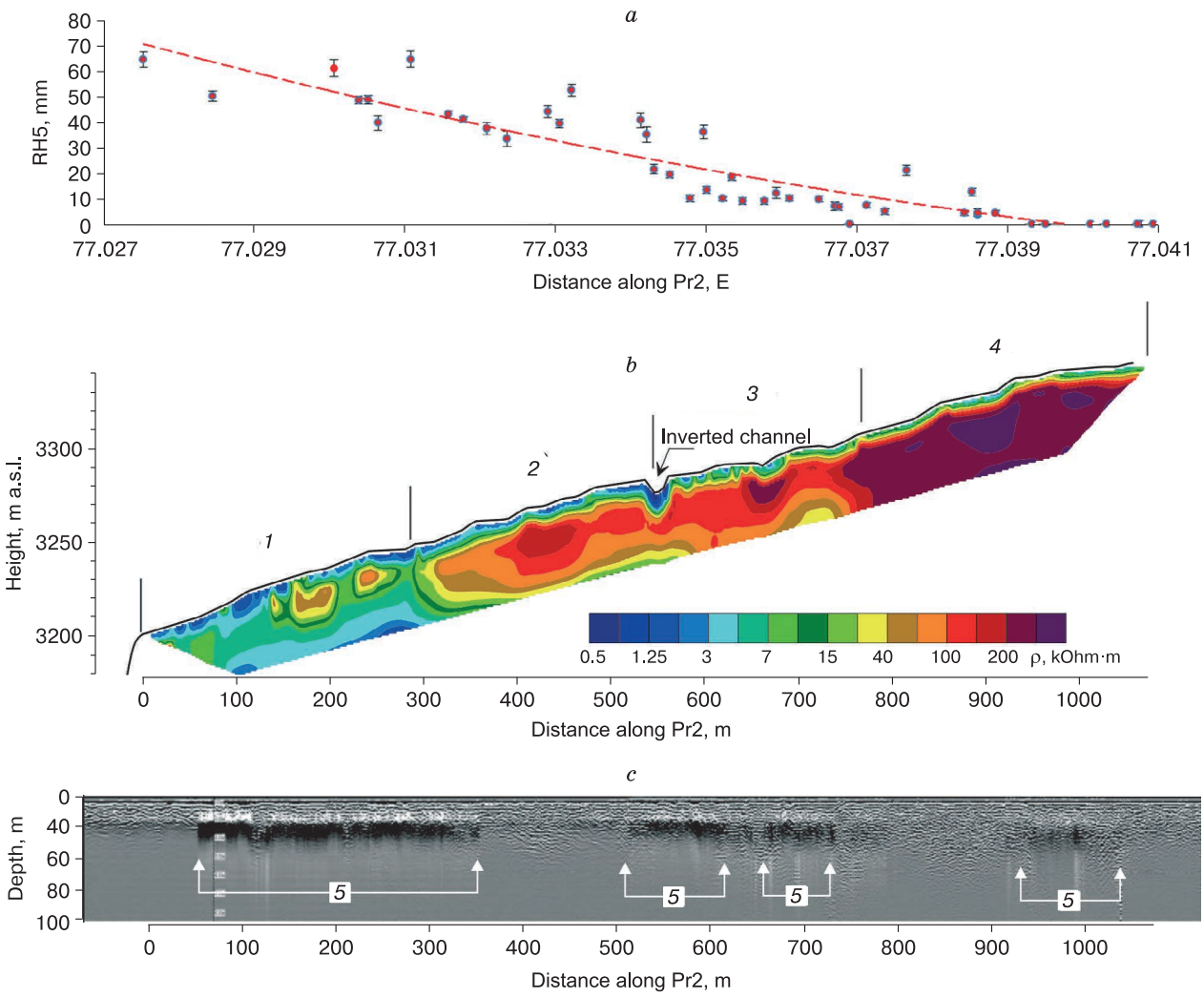

Fig. 3. A correlation between lichenometric index RH5 (*a*), geoelectric section (*b*) and GPR section (*c*) along the Pr2 profile laid along Gorodetsky rock glacier axis from the bar of its frontal slope:

a – index RH5 and trend line; *b* – electrical resistivity (ER) section; *c* – radio waves reflection pattern (GPR). The geoelectric section, various-age generations of the rock glacier are distinguished: *1* – lower (youngest): melted and the most highly dynamic; *2* – partly melted, with passive blocks of metamorphic ice; *3* – passive, late; formed by large blocks of metamorphic ice; *4* – inactive, formed by fields of metamorphic ice; thawed glacier bed. *5* – radio waves absorption areas, corresponding to zones of intensive water-logging at the level of the rock glacier bed.

The geoelectric section for the second generation is none the less heterogeneous. Thawed and ice-poor zones whose resistivity is lower than 80 kOhm·m account for about 60 % of the section volume. The remaining 40 % are formed by large, relatively monolithic frozen blocks with the resistivity reaching 100 kOhm·m and higher. Reduced resistivity of the bedrocks, as well as the GPR data indicate that the rock glacier bed is for the most part also thawed and locally strongly waterlogged. The third and other younger generations of the rock glacier located up the valley have resistivities averaging 100 kOhm·m and higher. The active layer distinctly distinguished by the ERT data has a thickness naturally tapering off from the front slope up the valley, while its resistivity increases from 0.5–1 to 3–7 kOhm·m. A decrease in ALT with increasing altitude is probably accounted for both high altitude climatic zones and for a greater number of massive blocks of metamorphic ice, grading from oldest to youngest generations of the rock glacier.

The differentiated resistivities in AL are accounted for the abundance of water-saturated fraction in the coarse debris material in the lower, oldest parts of the rock glacier, which generally reduces resistivity of the debris mantle. Whilst the coarse debris cover in the upper part of rock glacier is practically devoid of fine substrate, which prompts an in-

crease in resistivity. It should be noted that the ERT technique does not always enable reliable determination of thicknesses of large blocks of ice (e.g. if their dimensions are bigger than those of electrical prospecting tool (235 m)), nor detection of the water-logged glacier bed beneath them. This is largely due to the screening effect, when most of electric current flows through a relatively conductive active layer without penetrating into the insulator layer. However, the problem is resolved when the ERT and GPR data are interpreted jointly.

General overview of the analysis of geophysical survey results allowed to establish the following distinguishing features of Gorodetsky rock glacier structure:

1. The average resistivity tends to increase from the talus accumulation up along the rock glacier axis, which is indicative of increasing aggregate ice content in the rock glacier, whereas the temperature tends to decrease, and so does ALT, whilst its resistivity grows due to lower contents of substrate in the coarse debris cover.

2. The vertical and horizontal inhomogeneity of the geoelectric section implies a cellular structure of the two lower generations, where fossil blocks of metamorphic ice with high resistivity are encapsulated in the melted, strongly water-logged rock debris-gravel-loamy matrix.

3. The thickness of unconsolidated coarse debris cover with high resistivity consistently decreases from the glacier edge to its accumulation area.

4. Throughout the entire Pr2 profile, the rock glacier has a thawed, strongly water-logged bed, with the ongoing intensive filtration.

Runoff waters temperature regimes of active, passive and relict rock glaciers differ fundamentally and largely depend on the content of glacial ice [*Krainer, 2002; Krainer et al., 2007*]. The runoff water temperature of active glaciers containing a large amount of ice is not greater than 1 °C, while temperatures of meltwater of dead glaciers, whose ice is almost completely melted, tend to be higher than 1.7 °C [*Krainer et al., 2007*]. In addition, the runoff water temperatures of ice-rich glaciers are generally very stable, whereas those related to dead glaciers experience severe fluctuations caused by variations of air temperature and precipitation.

Accordingly, the 2013–2014 temperature monitoring of Gorodetsky rock glacier runoff water provided very unintuitive results [*Galanin et al., 2015; Galanin and Olenchenko, 2015*]. The authors installed three two-channel Hobo automatic loggers into three main meltwater underflow streams of the rock glacier (Fig. 1). Next to each logger, one temperature gauge was fixated by a sinker at the bottom of the stream channel at a distance of 2–3 m from the front slope base, while another gauge was attached to one of the large blocks at a distance of 50–60 cm from the water level. All the gauges were programmed for temperature recording at the interval of 3 hours.

Their readings were taken and analyzed in August 2014. Two loggers were found to be out of order due to containment failure (depressurization) during the freezing of watercourses, whereas one gauge was recording during the entire observation period. The raw geothermal data interpretation prompted the following inferences.

Active discharge of Gorodetsky rock glacier begins in the first decade of May and ends late in October, lasting for more than 5.5 months (Fig. 4, *a*). The runoff processes commence abruptly (over a span of 5–6 days), once positive average daily air temperatures are established. During the period of intense discharge between May 10 and October 10, the stream flow temperature averaged 1.7 °C from August 2013 to August 2014. The runoff water temperatures were gradually growing during the summer period and reached their maximum values (2.5 °C) by the end of July [*Galanin et al., 2015*]. During the two warmest months (July, August), meltwater temperature did not drop lower than 2.3 °C. Irregular temperature fluctuations with smooth, but large-amplitude (up to 0.5 °C) are observed in the first half of the runoff period. Beginning from August, the meltwater temperature stabilizes, with its amplitudes not exceeding 0.1 °C. The maximum mean monthly meltwater temperature showed a remarkable rise from 2.3 °C (August 2013) to 2.5 °C (August 2014). Whereas the sum of positive air temperatures in 2014 was significantly lower than in 2013 (Fig. 4, *a*). The data on the temperature regime of rock glacier discharge in the Alps [*Krainer et al., 2007*] whose temperature behavior is shown in Fig. 4, *b* indicate that it varies from 0 to 1 °C in active glaciers (ice content >80 % of the volume); does not exceed 1.7 °C in non-active (ice content <50 % of the volume); and persists above 1.7 °C in dead (relict) glacier (ice is melted). According to these data, Gorodetsky rock glacier should be ranked as a relict glacier (Fig. 4, *b*), since its runoff water temperature (2.3–2.5 °C) is significantly higher than temperature recorded in relict glaciers of the Alps. Besides, meltwater temperature of the Gorodetsky rock glacier correlates well with results of geophysical surveys, indicating thawed state of its frontal generation and low content of ground ice.

However, results of instrumental observations complemented by numerous proxies attest to Gorodetsky rock glacier being one of the most active in the region [*Gorbunov et al., 1992; Marchenko, 2003*].

Age of Gorodetsky rock glacier. The results of geophysical surveys and observations of natural outcrops bear the evidence that the upper, youngest and nevertheless most passive generation of Gorodetsky rock glacier abounds with large blocks of metamorphic ice inherited from older glacier during its degradation. In order to provide an accurate substantiation

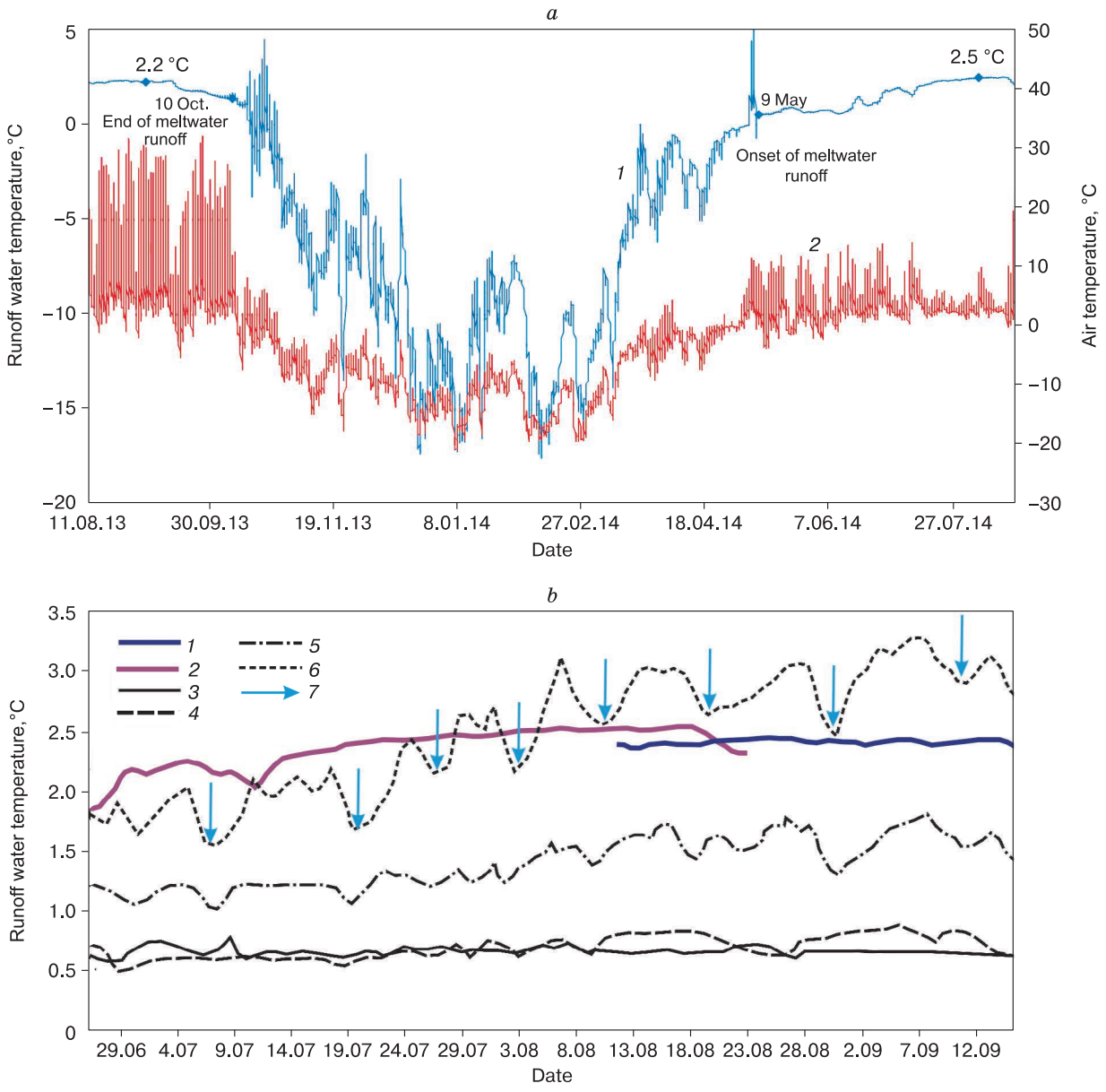

Fig. 4. Correlation between temperature regime of runoff flow of Gorodetsky rock glacier (*a*) and of rock glaciers with different activity in the Western Alps (*b*) after [*Krainer, 2002*].

a – variability of the runoff flow temperature (*1*) and surface air temperature (*2*) of Gorodetsky rock glacier from August 10, 2013 to August 20, 2014; *b* – correlation between meltwater temperatures of Gorodetsky rock glacier (*1* – 2013, *2* – 2014) and of glaciers in the Western Alps: *3* – Reichenkar (active); *4* – Kaiserberg (active generation), *5* – Suljar (inactive), *6* – Kaiserberg (dead generation); *7* – periods of heavy rains during observations in the Alps.

of the connection between late Holocene glaciers oscillations and formation of successive generations of rock glaciers in the region, it is critical to determine ages of the both.

Holocene glacial chronology of the Northern Tien Shan was reconstructed by *O.N. Solomina* and *O.S. Savoskul* [*1997*]. Relying primarily on lichenometric and radiocarbon dating, the authors established the following periods of glaciers advancement in the Northern Tien Shan: 1500–2000, 500–900, 200–400 and less than 100 years ago (BP). Moreover, terminal moraines of the first phase of the Little Ice Age (LIA) are found to occur 300–350 m below the current location of the glacier terminus. The area of glaciers shrunk in the middle of the Little Ice Age (400–150 yy BP), however their locations are reported 200–250 m below the current position [*Solomina and Savoskul, 1997*].

For relative and absolute age estimation of the Gorodetsky rock glacier surface, the authors employed lichenometric approach and the residual strength test, referred to as the Schmidt Hammer Test in the literature. The methodological aspects of this approach are well known and discussed in detail earlier [*Galanin and Pakhomov, 2010; Galanin et al., 2013*]. In tandem with R.A. Shakesby, J.A. Matthews, S. Winkler [*Matthews and Shakesby, 1984; Shakesby et al., 2004, 2006*], the authors used the mean value of five largest *Rhizocarpon* lichen specimens with yellow thallus from Rhizocarpon section (here and further in the text RH5 index, mm). To determine RH5 index, we investigated specimens from local populations at lichenometric sites, not more than 40 × 40 m in size, laid on morphologically homogeneous parts of the rock glacier.

Residual strength of the exposed surfaces (*Q*-value, %) was estimated using a Silver Schmidt rebound Hammer type N manufactured by Proceq (Switzer-

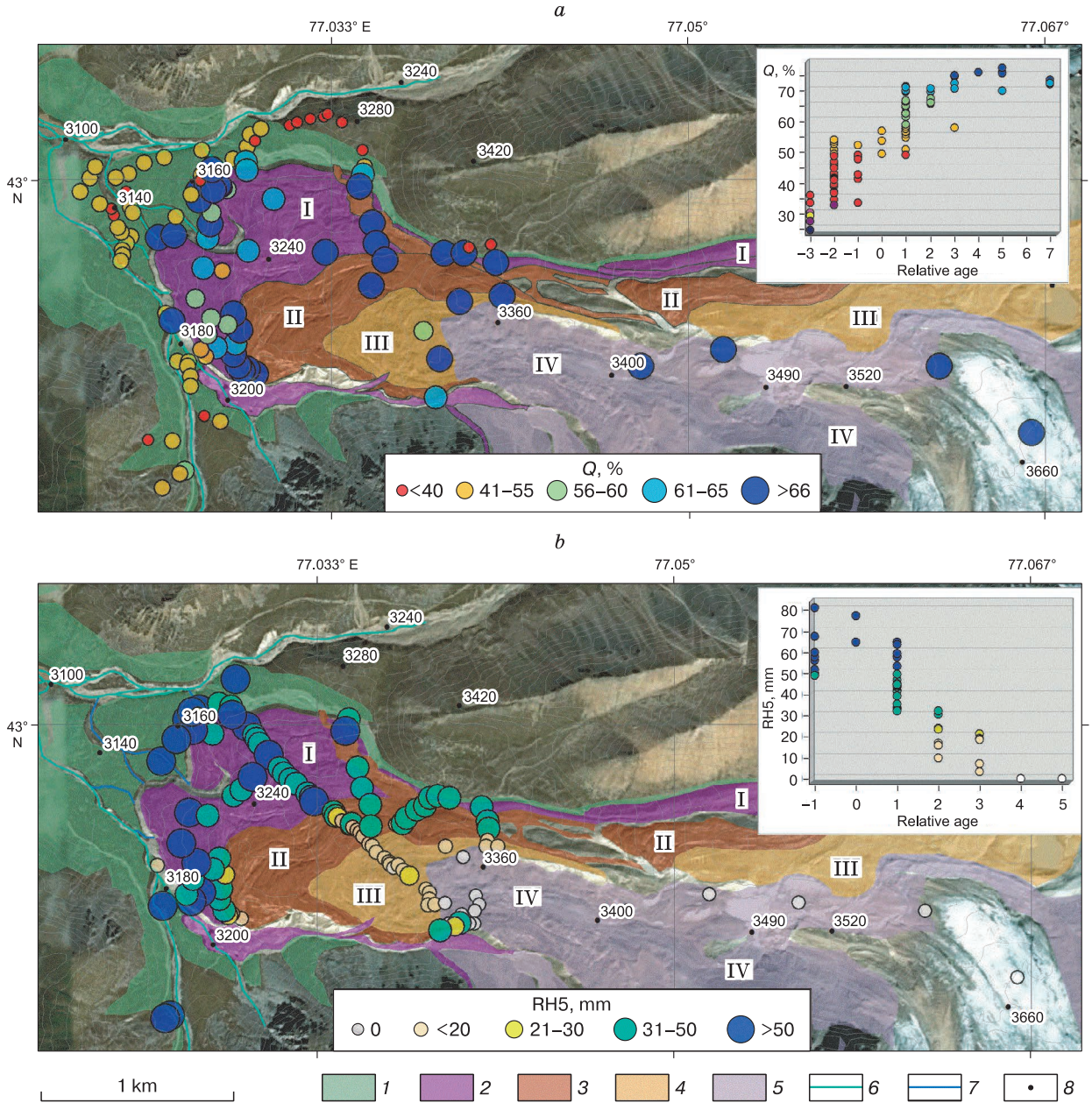

Fig. 5. Distribution of age indexed calculated from residual strength (*a*) and medial diameter of five largest *Rhizocarpon* sp. specimens (*b*) on the surface of Gorodetsky rock glacier.

1 – melted Early Holocene moraine; *2–5* – various-age generation of the rock glacier: *2* – phase I, LIA: 690 ± 80 BP; *3* – phase II, LIA: 340 ± 65 BP; *4* – phase III, LIA, 180 ± 60 BP; *5* – phase IV (ice moraine dated 20th century, with a large amount of metamorphic ice); *6* – watercourses; *7* – rock glacier discharge; *8* – elevation marks.

land), in parallel with lichenometric measurements at those same sites. *Q*-value was applied on the assumption that residual strength, calculated as a percentage of the rebound value, decreases as the debris become weathered and is dependent on their exposure time [*Goudie, 2006*]. When applying Schmidt hammer test, one should bear in mind that the exposed rocks can become fragmentarily rejuvenated due to their surface experiencing frost cracking and peeling off effect. The resulting lowest estimates of residual strength appear therefore more reliable than those with higher values. A total of more than 100 sites were set up within the Gorodetsky rock glacier area, of which some are located along geophysical profiles (Figs. 1, 5). At each site, 30–50 of the largest *Rhizocarpon* sp. thalli were investigated and measured. Whilst at sites with rare *Rhizocarpon* sp. all the encountered specimens were measured. To calculate RH5 value, we estimated the mean value of the five largest species.

At each site, from 70 to 200 anecdotal residual strength tests were conducted using a Schmidt hammer, with determination of their average value (*Q*-value). The testing was carried out on randomly selected 6–10 largest fragments of granitoid composition with a diameter of at least 0.5 m. The results of estimated *Q* and RH5 values are shown in Fig. 5. Next, we grouped and averaged the RH5 and *Q* values within each pre-determined generation of the rock glacier, and older moraines adjacent to it (Table 1). Heterogeneity of the surface rock glacier is most manifest in the extent the topsoil and vegetation cover and epilithic lichens are developed. The RH5 and *Q* values are found to be in stark contrast between the marginal generation and older moraine encroached upon by the rock glacier. These moraines are conditionally taken as zero generation (Table 1).

Given that the projective coverage of epilithic lichens reaches 80–90 % here, secondary successions are not rare. The lichenometric approach provides therefore only a minimal age estimate (Table 1). The value of RH5 = (59.33 ± 2.5) mm appears approximate in all moraines; while residual strength *Q*-value varies from (30 ± 4) % for the oldest moraine to (45 ± 6) % for the moraine closest to the glacier edge.

The oldest, 1st generation of rock glacier is characterized by a 40–70 % projective cover of epilithic lichens. Clusters of green mosses, graminous grasses and extremely rare small spruce up to 0.5 m high. The values of the indices RH5 = (47.52 ± 2.56) mm and *Q* = (62.8 ± 6.0) % significantly differ from those for the older moraines.

Unlike the first generation of the glacier, the second generation is characterized by higher values of residual strength (*Q* = (67.6 ± 6) %), although the confidence intervals of the estimates for both slightly overlap. The difference in ages between 1st and 2nd generations is remarkably reflected in sizes of epilithic lichens, inasmuch as the largest *Rhizocarpon* sp. on the surface of the 2nd generation are more than twice less in size (RH5 = (21.7 ± 1.7) mm).

The RH5 statistics is (10.47 ± 1.23) mm on the surface of conventional 3rd generation, while the projective coverage of epilithic lichens is not greater than 10 % there. Residual strength *Q* = = (69.10 ± 6.53) % differs only slightly from the previous generation. Within the bounds of the conventionally allocated 4th and 5th generations, which are the fields of "fossil ice" overlain by the cover of debris material, lichens *Rhizocarpon* sp. found to be nonexistent (RH5 = 0), while residual strength index reaches its maximum values of *Q* = 74–76 % (Fig. 5).

Table 1. **Distribution of mean residual strength values (*Q*), average value for five largest *Rhizocarpon* sp. Lichen (RH5) and age estimates of elements composing Gorodetsky complex rock glacier**

Component	Relative age (generation No.)	Number of *Q* measurements	*Q* ± err.	RH5	t_{RH5}, years BP	t_Q, years BP
Glacier and the adjacent ice-cored moraines						
Glacier terminus (debris cover)	5	195	74.83 ± 2.33	Lichens were not found	<43	
Terminal ice-cored moraine (debris cover)	4	75	76.20 ± 1.30		<43	
Rock glacier						
3rd generation (latest)	3	252	69.10 ± 6.53	10.47 ± 1.23	180 ± 60	
2nd generation (middle)	2	430	67.59 ± 5.24	21.74 ± 1.69	340 ± 65	
1st generation (earliest)	1	1963	62.80 ± 6.00	47.52 ± 2.56	690 ± 80	
Frontal slope foot	1	235	53.30 ± 3.50	47.40 ± 1.95	690 ± 70	
Early Holocene moraines (Preboreal stage)						
Basal moraine at the frontal slope-foot zone of glacier (erratic boulders)	0	474	45.31 ± 6.43	59.33 ± 2.50	860 ± 75	10 600–11 700
Talus accumulation of terminal moraine at a distance of 200–250 m from glacier terminus	0	2223	43.64 ± 4.48	Secondary successions		
Idem, at a distance of 400 m from glacier terminus	0	445	30.06 ± 3.76			

For estimation of minimum time t of the rock glacier surface exposure, the values of RH5 and Q require calibration. The equation for *Rhizocarpon* sp. growth in the periglacial zone of the Northern Tien Shan was substantiated by *O.N. Solomina* and *O.S. Savoskul* [*1997*] relying on the measurement of *Rhizocarpon* sp. lichens on moraines whose age was determined independently, by radiocarbon dating. The equation is written as

$$t_{RH5} = 43.2 + 13.2RH5 + 0.01RH5^2, \qquad (1)$$

where t_{RH5} is time of the surface exposure, years; RH5 is diameter of the largest *Rhizocarpon* sp. specimen, mm.

On the basis of equation (1), we converted RH5 values into absolute dates (Table 1), which generally correlate well with the LIA chronology of glacial events established by earlier research. The oldest generation (the marginal part) is thus dated 690 ± 80 BP. Its frontal slope position (3150 m a.s.l.) is 350–400 m lower than the glaciers edges in the source area of rock glacier, which agrees well with the data obtained by *O.N. Solomina* and *O.S. Savoskul* [*1997*], taking into account that the frontal slope position has somewhat lowered down over the last 80 years, as the glacier creeps down the valley at a rate of 1–2 m/year. The second generation of the rock glacier dated 340 ± 65 BP is located in the 3250–3300 m range of absolute elevations and correlates with the second phase of LIA. The third, latest and most passive generation of the glacier is dated 180 ± 60 BP. Its hypsometric interval (3300–3350 m a.s.l.) corresponds to the paleoglacier terminus position during the last phase of LIA.

The fourth and fifth generations being "fossil ice" fields armored with gravely debris cover, constitute the rock glacier source area, having no morphological features of the glacier movement. These impound the periglacial lakes and form the last marginal moraine resulted from the glaciers retreat during the second half of the 20th century. Lichens of the *Rhizocarpon* sp. taxon are totally missing there.

The minimum lichenometric age of the subglacial moraine (encroached upon by the rock glacier) is 860 ± 75 years. However, given that secondary successions of epilithic lichens and considerable weathering of the surface are strongly pronounced, this value is greatly underestimated. A more decrepit appearance of moraines attached to the rock glacier is also reflected in the residual strength value Q (30–45 %), which appears much less than the strength of debris on the glacier surface: (62.8 ± 6.0) % in the marginal part and (74.8 ± 2.3) % in its source area.

Close ranges of residual strength values Q = = (41.6 ± 1.4) % are established for Preboreal moraines composed of granitoids (granitic rocks) (11 700–10 640 BP) in Northern Norway [*Shakesby et al., 2004, 2006*], as well as for Pleistocene–Holocene glacial complexes of the Suntar-Hayat ridge (44.5 ± 6.1) % and (46.1 ± 6.5) % [*Galanin et al., 2013*]. Testing the younger moraines located further down the Bolshaya Almaatinka river valley showed that their residual strength does not drop below 30–35 %, regardless of their relative age. These Q values are likely to be the limiting values for encountered in this region rock morphosculptures composed of granitoids.

The residual strength method for age estimation deals with a remarkably larger timespan (thousands of years), unlike lichenometry (hundreds of years); nevertheless its resolution is an order of magnitude lower. From the results obtained, it follows that in climatic conditions of the periglacial zone of the Northern Tien Shan, the use of lichenometry is limited to 700–800 years, which is equivalent to lichens *Rhizocarpon* sp. 50–60 mm in diameter. In this time interval, the variation in residual strength Q value is probably not significant [*Goudie, 2006*].

The obtained results show that in the 0–2000 yy interval of LIA, the Q value permits to statistically reliably separate the oldest generations (Q = 55–65 %) from the contemporary ones (Q = 70–80 %). The Q value makes it possible to clearly differentiate early Holocene events ($Q << 50$ %) from those dated LIA ($Q >> 50$ %). These estimates are valid for rock morphosculptures composed of coarse-grained granitoids.

Assuming that moraines in the frontal part of Gorodetsky rock glacier are at least 10,000 to 11,000 years old, and the linear relationship between the residual strength and exposure time [*Shakesby et al., 2004, 2006; Winkler, 2005; Goudie, 2006*], we analyzed the regression Q/t, which is approximated by equation

$$Q = -6.772 \ln (t_Q) + 103.48,$$

where t_Q is absolute age, years. This equation requires additional verification, though. However, taking into account the above limitations, it can be used for rough estimation of the absolute time of exposure of rock surfaces, granitoid in composition, in this region.

Study of the isotope composition of fossil ice and meltwater runoff. In recent decades, the study of the stable isotope ratios in the ice of rock glaciers has become an integral part of the methodological arsenal in most foreign research [*Stauffer and Wagenbach, 1990; Cecil et al., 1998; Steig et al., 1998; Krainer et al., 2007*]. Unfortunately, there is no information on the stable isotope ratio for rock glaciers of Russia and FSU countries (after [*Vasilchuk Yu.K. and Vasilchuk A.C., 2011*]).

In August 2013, the authors studied two meltwater samples from Gorodetsky rock glacier collected at the geothermal loggers location points (Fig. 1, OP 33, 34), two samples from a fossilized block of metamorphic ice in the middle part of the rock glacier (OP 71) and two samples of firn ice from the mar-

Table 2. **The isotopic composition of runoff water and fossil ice of Gorodetsky rock glacier, Zailiyskiy Alatau**

Sample types	Depth, m	*N*	$\delta^{18}O$	δD	d_{exc}	$\delta D/\delta^{18}O$
Subglacial runoff beneath rock glacier (OP 33, 34)	20	2	−12.54 ± 0.01	−85.78 ± 1.86	14.51	6.84
Lens of metamorphic ice from permafrost (OP 71)	5	2	−13.75 ± 0.01	−93.10 ± 0.05	16.91	6.77
Ice from glacier's marginal part (OP 83)	2	1	−12.99	−87.45	16.47	6.73
Ice from glacier surface (OP 85)	0	1	−13.14	−95.19	9.93	7.24
Average			−13 ± 1	−90 ± 4	15 ± 3	6.9 ± 0.2

Note. *N* is the quantity of the analyzed samples.

ginal part of Gorodetsky glacier (OP 83, 85). The sampling points are shown in Fig. 1, and the results of their isotopic analysis are given in Table 2 showing that the stable isotope ratios in all the analyzed samples are almost identical. The $\delta^{18}O$ variability constituted −10...−14 ‰, and that of δD equaled −85...−95 ‰. Stable isotope ratios and high positive deuterium excess (d_{exc} = 10–16) suggest the atmospheric origin of the composition of the studied samples, and their great similarity to the metamorphic ice melts in the contemporary glaciers in the region (Fig. 6).

The affinity between the isotope compositions of rock glacier runoff waters and metamorphic ice in the glacier source areas may indicate the absence of any other sources of water during sampling, rather than the melting metamorphic ice. On the one hand, this implies a great number of blocks of metamorphic ice, established by geophysical methods and visual observations, and attests to negligible volumes of other ice (otherwise, as a result of the glacial and ground ice melts mixing, the total isotope of the rock glacier runoff water would have undergone a significant change in the composition due to the dilution processes). On the other hand, a very light isotope composition of meltwater may be indicative of the still poorly studied isotope fractionation processes occurring during the flow filtration through the glacier mass cooled to zero temperatures. As such, heavy water accumulating in the pores and on rock fragments as infiltration ice, can start to freeze out at temperatures as high as +1...+2 °C (the deuterium water freezing point is +3.4 °C), enriching thereby the draining residual meltwater with light isotopes. The similar inferences were made by Yu.K. Vasil'chuk and his colleagues upon proceeding the laboratory experiments on partially freezing/thawing water samples [*Vasil'chuk et al., 2006*].

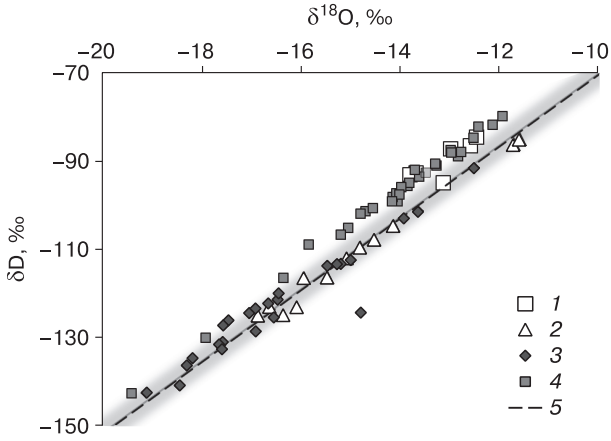

Fig. 6. Isotopic composition of meltwater and fossil ice of Gorodetsky rock glacier compared with compositions of several other types of ice.

1 – water runoff and metamorphic ice of Gorodetsky glacier (August 2013); *2, 3* – discharge of rock glaciers of the Gorny Altai in the Sophia glacier valley in August 2014 (*2*) and in July 2015 (*3*); *4* – metamorphic ice from various-aged moraines and from the surface of the Bolshoy Azau glacier (Caucasus) [*Vasil'chuk et al., 2006*]; *5* – equilibrium line of meteoric waters of Craig glacier ($\delta D = 8.13\delta^{18}O + 10.8$).

The available in foreign literature research results on rock glaciers indicate that the isotopic composition of ice composing them is analogous to modern glaciers. Thus, ice sampled from the metamorphic ice-core of Reichenkar rock glacier (2300–2700 m a.s.l.) in the Alps is characterized by the presence of winter (light weighing) and summer (heavy) interlayers of ice, whose $\delta^{18}O$ value varies from −12 to −17 ‰ [*Krainer et al., 2007*]. In these mountains, the $\delta^{18}O$ value for metamorphic ice of Chli Titlis glacier ranges between −13 and −16 ‰ [*Lorrain and Haeberli, 1990*]. Similar data were obtained for ice samples from the ice-core of Galen Creek rock glacier (2700 m a.s.l.) in the Cordilleras, where the $\delta^{18}O$ value ranges from −15 ‰ (summer layers) to −19 ‰ (winter layers). The average $\delta^{18}O$ value for core samples from Inylchek glacier (the largest in the Central Tien Shan) in the 4100–4400 m a.s.l. altitude interval constitutes −15 ‰, while for summer precipitation (snow and rain) it is about −7 ‰ [*Aizen V. and Aizen E., 1996*]. Inasmuch as the isotopic composition tends to grow lighter with altitude, it can be assumed that $\delta^{18}O$ value for the lower-altitude Tien Shan glaciers equals −12...−14 ‰.

Thus, the $\delta^{18}O$ content in the ice-cores of rock glaciers is identical to the marginal parts of modern glaciers from the same mountain regions, which serves as one of the indications of a close genetic affinity between them [*Vasilchuk Yu.K. and Vasilchuk A.C., 2011*]. More profound insights about rock glacier structure and genesis are likely to be made from dedi-

cated studies of their runoff, whose isotope composition is subject to appreciable changes during the summer period [*Krainer et al., 2007*]. The $\delta^{18}O$ content in five simultaneously studied rock glaciers in the Alps, was thus found to be very close, which tended to gradually increase from –18 to –13 ‰ in the period from May through October [*Krainer et al., 2007*]. The increasingly heavier composition of meltwater during the runoff period agrees quite well with the understanding of fractionation during the slow melting metamorphic ice, firn and snow, which is also established experimentally [*Taylor et al., 2002*]. It should be admitted that the mechanisms for natural fractionation of the isotopic composition of ice and water inside rock glaciers are still poorly understood, representing therefore an important direction for near-future research.

DISCUSSION

The results of a comprehensive study of Gorodetsky rock glacier appear to overthrow the present concepts of structure, origin and rheology of rock glaciers in general. According to these, rock glaciers are monolithic-frozen bodies consisting of a coarse clastic matrix cemented predominantly by ground ice [*Gorbunov and Titkov, 1989; Barsch, 1996; Galanin, 2009*], that move due to the visco-plastic deformations substantiated by J. Glen [*Glen, 1952; Haeberli, 1985; Barsch, 1996*]. In reality, there is still a paucity of field data on the internal structure of rock glaciers. In this respect, Murtel 1 is the best studied rock glacier in the Alps, where according to W. Haeberli et al. [*Haeberli, 1985; Haeberli et al., 2006*] three deep (>50 m) and several shallower (5 to 10 m) wells have been drilled [*Barsch, 1996*].

A deep well drilled by W. Haeberli and his colleagues [*Haeberli, 1985*] with an aim to prove the glacial origin of the rock glacier, penetrated up to 12 m thick layer of pure metamorphic ice subjacent to a loose, gravely-blocky surface layer. The rest of the section was composed of stratified sediments represented by alternating sand loams, clay loams and sandy-gravely-silty horizons with low amount of snow. The glacier bed temperature was found to be close to zero. The boreholes drilled by *D. Barsch* [*1996*], who insisted on solely permafrost origin of rock glaciers, exposed fundamentally different sections. He did not find any metamorphic ice, though, which attests to their ties with glaciers. Beneath the loose, gravelly-blocky debris cover the drilling exposed alternating frozen sandy loams, clay loams, intercalations of pebble and well-sorted gravel, and icy layers with thickness not more than 1–2 m.

A significant disagreement with the drilling results obtained by *D. Barsch* [*1996*] is explained by the destruction of initial structure of core-samples while drilling into the rock glaciers. Ice cement partially or completely melts when the ice-gravelly layers with temperatures close to zero are being drilled through. This insight seems to be rather speculative, inasmuch as the data resulted from the comprehensive geophysical surveys conducted by *W. Haeberli* [*1985*] which included density gamma-ray logging, unambiguously testify to the two-member structure of the glacier and to the presence of extensive deposits of fossil metamorphic ice in its upper part. The available direct data on rock glaciers structure have thus far not confirmed any presence of a layer of monolithically ice-cemented gravelly-blocky deposits in their sections. However, both the definition of and understanding about the mechanisms for rock glaciers movement ascertain that these are interpreted to be basic constituent of the upper part of their sections.

The results of electrical sounding and GPS surveys, and high temperatures of Gorodetsky rock glacier runoff waters corroborate the hypothesis about the absence of a consolidated frozen structure in this portion of the glacier. Whilst the most active marginal generations (periglacial environments) of the rock glacier are dominantly in the thawed state throughout their entire sequence (30–40 m). The latest (younger) generation of the rock glacier, not revealing features of plastic deformations, contain large blocks of fossil metamorphic ice, loosely bound together as partially frozen gravelly-blocky patches. The large blocks of ice are more likely to be inherited from the ancient glacier rather than associated with their origination inside rock glacier, which is also confirmed by their isotopic composition, stratigraphic features and the nature of plastic deformations. The age estimates for Gorodetsky rock glacier also support its historical-genetic affinity with the paleoglacier, whose shrinking episodes would result in the subsequently forming next generations of the rock glacier, which pre-existed as the fields of “fossil ice”, separated by small periglacial lake basins where seasonal varve clay loams tended to accumulate. Basically, these generations acted as dams and impounded the glacial runoff system.

The authors have reliably established that the amount of ice in Gorodetsky rock glacier tend to be abruptly decreasing, beginning from the younger (upper) to the ancient (marginal) generations. However, relying on the widely accepted concept of ice in rock glaciers being the most plastic element that dictates their creep, then the frontal generations of Gorodetsky rock glacier should be ranked among the most passive generations. The synthesis of a whole complex of instrumental observations of the Gorodetsky rock glacier commenced in 1923 by N.N. Palgov, and then succeeded in 1990–2000 by V.A. Zenkova, A.P. Gorbunov, S.N. Titkov [*Gorbunov et al., 1992*], and by *S.C. Marchenko* [*2003*], has allowed the following inferences (Fig. 7): during the period spanning 77 years, the glacier’s frontal slope crept 72 m

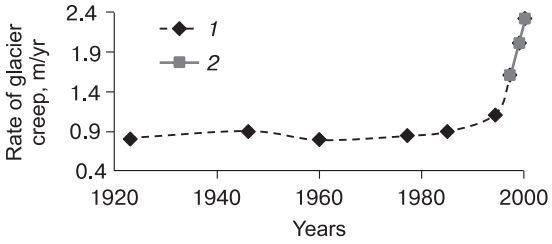

Fig. 7. Maximal multiyear rates of the frontal slope movement of Gorodetsky rock glacier based on the reference point observations.

1 – data obtained by N.N. Palgova, V.A. Zenkova, A.P. Gorbunov, S.N. Titkov [*Gorbunov et al., 1992*]; *2* – data obtained by *S.S. Marchenko* [*2003*].

down the valley. The different lobes of its front moved at different speeds, periodically running ahead of and catching up with each other. The average multi-year speed in the period from 1940 to 2000 showed about 3-fold increase (from 0.9 to 2.6 m/year). Over the same time period, the glaciers termini retreated by 200–250 m in the accumulation area, while the temperature increased substantially and the lower boundary of the permafrost belt rose higher. An active advancement is also reported for the morphologically identical Morenny glacier [*Glazovsky, 1977; Cherkasov, 1989*], located 3 km from Gorodetsky rock glacier, as well as most other glaciers distinguished in the region and confined to different hypsometric intervals. Moreover, their movement activation can not be associated with the head pressure of glaciers located higher, since the latter were increasingly shrinking during this period [*Glazovsky, 1977*].

According to *S.S. Marchenko* [*2003*], the most active in the study area is Burkutta rock glacier, whose maximum movement rate increased from 5 to 14 m/year from 1979 to 1984. The glacier receded by 100 m in its source area between 1969 and 1984, though. In the next decade (1987–1997), the advancement rate of the glacier frontal slope slowed down to be "back to square one", at a rate of 5 m/year [*Marchenko, 2003*]. The integration of the data obtained allows to outline a possible mechanism for movement of such glacial formations, realized in the context of current climate changes and degradation of the alpine glaciation. Initially, the next generation of a rock glacier evolves against the backdrop of the ongoing drastic climatic changes and rapidly rising firn boundary at the glacier transition across the equilibrium line, to the negative mass balance. In this case, the ablation zone tend to prograde up the glacier, establishing thereby the characteristic concave-upward transverse profile of the marginal part. Redistribution of the surface glacial runoff towards the thalweg leads to a rapid incision of newly formed thermo-erosion canyons and aggradation of a new field of "passive" ice in the marginal part. These tend to slowly degrade and eventually become draped with gravelly-block cover of the ablation moraine. Concurrently, a wide range of cryogenic processes are activated within the layer of annual thermal cycle: polygonal cracking of metamorphic ice blocks, frost sorting of debris cover, thermo-erosion and suffosion. Given a large number of vertical cracks, the suprapermafrost waters are filtered through to the bedrock base. The filtration processes, in turn, lead to intense lateral and subsurface thermo-erosion of ice blocks. This gradually produce surfaces of the fields of "passive" ice that have chaotic bumps and pits, eventually forming thereby inversion mesorelief, within which a partial redistribution of the surface moraine into thermokarst depressions resulting from the debris flow, deserption and solifluction processes.

Some specific valley configurations determine the conditions, when the overlying glacier runoff is partially or completely blocked and begins to drain through the moraine, while the process intensify provokes degradation of the buried blocks of metamorphic ice. The void space is progressively filled with finely dispersed material ("glacial flour"), abundantly arriving with the glacial runoff. The active precipitation of "glacial flour" in the bodies of some rock glaciers is confirmed by comparing the degree of turbidity of their meltwaters with that of glaciers. The glacier runoff waters are intensely saturated with suspended particles and their apparent turbidity reaches 800–1000 NTU (nephelometric units) and more. The rock glaciers meltwater is characterized by high transparency, whose turbidity does not exceed 40–60 NTU. Given that the entire glacial runoff is filtered through the rock glacier, it becomes evident that the bulk of suspended clay-loams accumulates inside its volume. This process is very likely to be developing in many glacial regions of Europe and Asia against the backdrop of increasingly accelerated ablation. The finely dispersed material contributed to the glacier runoff becomes the main source of terrigenous material for many periglacial glaciers.

As a result of these processes, the structure and physical properties of the rock glaciers have strikingly changed. The main plastic elements of their movement thus become represented not by blocks of fossil ice or ice-cement, but by melted highly waterlogged clay-loamy material, filling pores and voids and possessing exceptional thixotropic properties. In addition, the total mass of the rock glacier and the bulk density tend to simultaneously increase, exerting thereby heavier loading on the glacier bed. The movement of such glaciers does not obey the Newtonian viscous flow of J. Glen's flow law. The difference between Newtonian and non-Newtonian "flows" consists in the fact that viscosity of the former is constant and does not depend on the speed of movement,

while in case of the latter, viscosity can decrease significantly or, conversely, increase with the increased rate of glacier creep. The thixotropic flow behavior is non-Newtonian either, as these liquids become even more diluted during acceleration of their motion, which, in turn, accelerates the movement even more. Among the known non-Newtonian fluids are non-hardened cement, concrete and many others. Consisting of a mixture of different fine particles, non-Newtonian fluids are therefore not monomolecular.

CONCLUSIONS

Results of the comprehensive study of Gorodetsky rock glacier allowed the following conclusions:

1. Given that the rock glacier does not have a consolidated frozen structure throughout its entire length, technically, it is not capable of moving due to viscoplastic deformations of the ground ice, according to Glen's flow law. The bulk of the rock glacier is composed of fossil blocks of metamorphic ice, inherited from the paleo-glacier.

2. The rock glacier consists of three variously aged generations that correlate well with the late Holocene oscillation episodes of mountain glaciers of the Northern Tien Shan.

3. The stable isotopic composition of meltwater flow of the rock glacier and fossil blocks of metamorphic ice show a great similarity to the composition of firn ice of modern glaciers.

4. The most active lower generation of rock glacier is found to be in the melted and highly waterlogged state; the volume of ground ice is almost non-existent in its structural composition.

5. The rock glacier structure does not fit well into the classical definitions of such formations; and given the ground ice deformations, the movement character of its monolithic body does not obey laws of viscoplastic flow, either.

6. The obtained data highlight that Gorodetsky rock glacier and, probably, many other super-active rock glacier from the region represent by themselves partly melted ice-rock – clay-loamy formations whose sliding is governed by the principle of thixotropic liquids, which explains sudden accelerations in their movement (surges), specific surface relief reminding of concrete-flow deformations, hydrodynamic discontinuities and suddenly occurring fast-moving ice-mud-rock mudflows.

This paper includes materials and results of the 2013–2014 field research conducted with support from Kasakhstan Geography Institute and, personally, the Director, prof. A. Medeu, its staff, and E.V. Severskiy, Head of the Laboratory for high-mountain permafrost, Melnikov Permafrost Institute SB RAS.

The work was funded by the Russian Foundation for Basic Research (Projects No. 11-05-00318-a, 14-05-0043514).

References

Aizen, V., Aizen, E., 1996. Isotopic measurements of precipitation on central Asian glaciers (southeastern Tibet, northern Himalayas, central Tien Shan). J. Geophis. Res. 101 (D4), 9185–9196.

Barsch, D., 1996. Rockglaciers. Springer-Verlag, Berlin, 331 pp.

Cecil, L.D., Green, J.R., Vogt, S., Michel, R., Cottrell, G., 1998. Isotopic compositions of ice cover and meltwater from the upper Fremont Glacier and Galena Creek Rock Glacier, Wyoming. Geografiska Ann., No. 80A, iss. 3–4, 287–292.

Cherkasov, P.A., 1989. Dynamics of Nizkomorenny rock glacier in the Dzhungar Alatau over 35 years, in: Ledniki, snezhny pokrov i laviny v gorakh Kazakhstana (Glaciers, Snow cover and Avalanches in the Mountains of Kazakhstan). Alma-Ata, Nauka, pp. 180–216. (in Russian)

Fabre, D., Francou, B., Jomelli, V., Kaiser, B., Arnaud, Y., Pouyaud, B., Smiraglia, C., Valla, F., 2001. Analyse de la structure d'un glacier rocheux du domaine tropical (Caquella, Sud Lipez, Bolivie). La Houiile Blanche, vol. 3–4, 124–132.

Farbrot, H., Isaksen, K., Eiken, T., Kaab, A., Sollid, J.L., 2005. Composition and internal structures of a rock glacier on the strandflat of western Spitsbergen, Svalbard. Norsk Geogr. Tidsskr – Norwegian J. Geography, vol. 59, 139–148.

Francou, B., Fabre, D., Pouyaud, B., Jomelli, V., Arnaud, Y., 1999. Symptoms of degradation in a tropical rock glacier, Bolivian Andes. Permafrost and Periglacial Processes, 10 (1), 91–100.

Frolov, A.D., 1998. Electric and Elastic Properties of Frozen Rocks and Ice. ONTI PNTs RAN, Pushchino, 515 pp. (in Russian)

Galanin, A.A., 2009. Rock glaciers in northeastern Asia: mapping and geographical analysis. Kriosfera Zemli, XIII (4), 49–61.

Galanin, A.A., 2010. Rock glacier: issues of terminology and classification. Vestn. SVNTs DVO RAN, No. 4, 2–11.

Galanin, A.A., Lytkin, V.M., Fedorov, A.N., Kadota, T., 2013. The Reduction of Glaciers Extent on the Suntar-Khayata Mts and Methodical Aspects of its Estimation. Led i Sneg, 53 (4), 30–42.

Galanin, A.A., Olenchenko, V.V., 2015. The new genetic type of super dynamic rock glaciers in Central Asia. General, Regional and Historical Geocryology Intern. Conf. "Permafrost in XXI century: basic and applied researches". Pushchino, Russia, pp. 113–114.

Galanin A.A., Olenchenko, V.V., Khristoforov, I.I., 2015. New data on the internal structure, hydrological regime and rheology of rock glaciers of the Northern Tien-Shan, the sources of catastrophic glacial debris flows, in: Fundamental and Applied Issues in Geocryology: Proceed. of the 21st Conference on ground waters of Siberia and the Far East. IMZ SO RAN, Yakutsk, pp. 369–375. (in Russian)

Galanin, A.A., Pakhomov, A.Yu., 2010. Case history of using the "Oniks 2.6.2" Sclerometer for dating of the Mandychan complex (Chersky Ridge). Geomorfologia, No. 1, 16–25.

Glazovsky, A.F., 1977. Rock glaciers of the Bolshaya Almaatinka River basin (ZailiyskiyAlatau), in: Cryogenic phenomena of high mountains. Nauka, Novosibirsk, pp. 85–92. (in Russian)

Glen, J.W., 1952. Experiments on the deformation of ice. Glaciology, No. 2, 111–114.

Gorbunov, A.P., Titkov, S.N., 1989. Rock Glaciers of the Cental Asian Mountains. IMZ SO RAN, Yakutsk, 164 pp. (in Russian)

Gorbunov, A.P., 2006. Rock glaciers in Asia outside Russia. Kriosfera Zemli, X (4), 19–28.

Gorbunov, A.P., 2008. Rock glaciers of the world: A review (Report 3). Kriosfera Zemli, XII (4), 14–23.

Gorbunov, A.P., Severskiy, E.V., 2000. The largest complex rock glacier in the Tien-Shan. Geomorfologia, No. 3, 48–54.

Gorbunov, A., Titkov, S., Polyakov, V., 1992. Dynamics of rock glaciers of the Northern Tien-Shan and the Djungar Alatau. Permafrost and Periglacial Processes, vol. 3, 29–39.

Goudie, A.S., 2006. The Schmidt Hammer in geomorphological research. Progress in Phys. Geography, No. 30, 703–718.

Haeberli, W., 1985. Creep of mountain permafrost: internal structure and flow of alpine rock glaciers. Mitteilungen der Versuchsanstalt fer Wasserbau. Hydrologie und Glaziologie. Zurich, vol. 77, 142 pp.

Haeberli, W., Hallet, B., Arenson, L., Elconin, R., Humlum, O., Kääb, A., Kaufmann, V., Ladanyi, B., Matsuoka, N., Springman, S., Vonder Mühll, D., 2006. Permafrost Creep and Rock Glacier Dynamics. Permafrost and Periglacial Processes, vol. 17, 189–214.

Iveronova, M.I., 1950. Rock glacier in the Northern Tien Shan, in: The Tien Shan physico-geographical Station Works, Issue 1, pp. 69–88. (in Russian)

Kneisel, C., Hauck, C., Fortier, R., Moorman, B., 2008. Advances in geophysical methods for permafrost investigations. Permafrost and Periglacial Processes, vol. 19, 157–178.

Krainer, K., 2002. Hydrology of active rock glaciers: examples from the Austrian Alps. Arctic, Antarctic and Alpine Res., No. 34 (2), 142–149.

Krainer, K., Mostler, W., Spötl, C., 2007. Discharge from active rock glaciers, Austrian Alps: a stable isotope approach. Austrian J. Earth Sciences, vol. 100, 102–112.

Loke, M.H., 2009. Electrical imaging surveys for environmental and engineering studies. A practical guide to 2-D and 3-D surveys, RES2DINV Manual, IRIS Instruments. – URL: http:.www.iris-instruments.com/Support/support.html

Lorrain, R., Haeberli, W., 1990. Climatic change in a high-altitude Alpine area suggested by the isotopic composition of cold basal glacier ice. Ann. Glaciology, vol. 14, 168–171.

Marchenko, S.S., 2003. Permafrost Zone of the Nothern Tien-Shan: past, present, and future. IMZ SO RAN, Yakutsk, 106 pp. (in Russian)

Matthews, J.A., Shakesby, R.A., 1984. The status of the "Little Ice Age" in southern Norway: relative age dating of Neoglacial moraines with Schmidt Hammer and lichenometry. Boreas, No. 13, 333–346.

Maurer, H., Hauck, C., 2007. Instruments and methods geophysical imaging of alpine rock glaciers. J. Glaciol. 53 (180), 110–120.

Palgov, N.N., 1957. Observations on the advance of one of the rock glaciers of the Djungar Alatau ridge. Izv. AN KazSSR. Ser. geol., iss. 2, 195–207.

Recommendations on the integration of geophysical methods applied to permafrost surveys, 1987. PNIIIS, Stroiizdat, Moscow, 88 pp. (in Russian)

Shakesby, R.A., Matthews, J.A., Winkler, S., 2004. Glacier variations in Breheimen, southern Norway: relative-age dating of Holocene moraine complexes at six high-altitude glaciers. The Holocene, 14 (6), 899–910.

Shakesby, R.A., Matthews, J.A., Owen, G., 2006. The Schmidt hammer as a relative-age dating tool and its potential for calibrated-age dating in Holocene glaciated environments. Quatern. Sci. Rev. 25 (21–22), 2846–2867.

Solomina, O.N., Savoskul, O.S., 1997. Glaciers on the western and northern periphery of the Tien-Shan over 2000 years. Geomorfologia, No. 1, 78–86.

Stauffer, B., Wagenbach, D., 1990. Stable isotopes, in: Pilot analyses of permafrost cores from the active rock glacier Murtèl, Piz Corvatsch, Eastern Swiss Alps: A Workshop Rep. W. Haeberli (Ed.). Arbeitsheft VAW/ETHZ, vol. 9, pp. 22–23.

Steig, E., Fitzpatrick, J., Potter, N., Clark, D.H., 1998. The geochemical record in rock glaciers. Geografiska Ann. 80A (3–4), 277–286.

Taylor, S., Feng, X., Williams, M., McNamara, J., 2002. How isotopic fractionation of snowmelt affects hydrograph separation. Hydrol. Processes, 16 (18), 3683–3690.

Vasil'chuk, Yu.K., Chizhova, Yu.N., Papesh, V., Budantseva, N.A., 2006. Stable isotopic composition of the ice of Bolshoi Azau valley glacier tongue, Mt. Elbrus area. Kriosfera Zemli, X (1), 56–68.

Vasil'chuk, Yu.K., Vasil'chuk, A.C., 2011. Isotope Ratios in the Environment. Part I: Stable isotope geochemistry of natural ice: Textbook. Moscow University Press, Moscow, 228 pp. (in Russian)

Vilesov, E.N., Gorbunov, A.P., Morozova, V.N., Severskiy, E.V., 2006. Degradation of glaciation and cryogenesis of modern moraines in the Northern Tien Shan. Kriosfera Zemli, X (1), 69–73.

Vladov, M.L., Starovoitov, A.V., 2004. Introduction to Ground Penetrating Radar: Textbook. Moscow University Press, Moscow, 153 pp. (in Russian)

Winkler, S., 2005. The Schmidt hammer as a relative-age dating technique: potential and limitations of its application on Holocene moraines in Mt Cook National Park, Southern Alps, New Zealand. New Zealand J. Geol. and Geophys., vol. 48, 105–116.

Received December 20, 2015